Large-Signal Modeling of GaN FET and Nonlinearity Analysis Using Volterra Series

Syed S. Islam and A. F. M. Anwar

Department of Electrical and Computer Engineering, University of Connecticut
260 Glenbrook Road, Storrs CT 06269-2157, anwara@engr.uconn.edu

Abstract – **A large-signal model is reported to investigate the nonlinearities of a GaN MESFET. The model developed accounts for the observed current collapse and frequency dispersion of output resistance and transconductance and uses Volterra series technique to determine the nonlinearities. Calculated f_T and f_{max} of a 0.8 μm x 150 μm GaN MESFET are 6.5 GHz and 13 GHz, respectively, and are in close agreement with their measured values of 6 GHz and 14 GHz, respectively. For a 1.0 μm x 150 μm FET operating at 1 GHz, 1-dB compression point and output referred third-order intercept point (OIP3) are 18 dBm and 25.3 dBm, respectively. The corresponding quantities are 19.6 dBm and 30.5 dBm for a 0.6 μm x 150 μm FET at same frequency. Similar improvements in third-order intermodulation (IM3) for shorter gate length devices are reported.**

I. INTRODUCTION

Recently, GaN based devices are extensively pursued for potential applications in high power microwave circuitries. GaN with a bandgap of 3.4eV, saturation velocity of 3×10^7 cm/s, low field mobility of 1500 cm^2/V.s and low parasitics is suitable for high power and high frequency applications. GaN grown on SiC offers a thermal conductivity of 4.5 W/cm/K making the system applicable for high temperature and high power applications. GaN HEMTs with output power of 9.8 W/mm at 8 GHz [1], f_T = 101 GHz and f_{max} = 155 GHz [2], and operating temperature of 750C [3] have been reported. However, GaN based devices are plagued with traps that lead to current collapse in the I-V characteristics [4-6] and frequency dispersion of output resistance and transconductance as has been observed in their GaAs counterparts [7-8]. Current collapse is observed in the absence of light and at high drain bias and is associated with the trapping of electrons at the channel/buffer interface. Current collapse is dependent on the time-interval between measurements of successive traces of I-V characteristics. With increasing time-interval between measurements current collapse is recovered due to detrapping of electrons [5]. This relates trapping effects with the applied signal frequency and can be modeled by the frequency dispersion of device transconductance and output resistance [7-8]. The large-signal device models must include dc to RF dispersions of the device characteristics for accurate analysis of the analog and mixed signal and high power circuits [7-8].

In this paper, a large-signal circuit model for GaN MESFET is presented that takes into account the effect of traps. Intrinsic model parameters are calculated using physics-based analyses. Device nonlinearities have been calculated using Volterra series analysis for possible application in power amplifiers.

II. ANALYSIS

The large-signal GaN MESFET circuit model is shown in Fig.1. The carriers captured by the traps located at the channel/substrate interface form a depletion layer inside channel that affect the drain current. The drain current considering this depletion layer is expressed in a modified form of the current equation reported by Klein *et al.* [4] as:

$$I_D = \frac{qN_d\mu_n Wd}{L}\left\{V_{DS} - \frac{2}{3}\sqrt{\frac{2\varepsilon}{qN_d d^2}}\left[(V_{bi}+V_{DS}-V_{GS})^{\frac{3}{2}} - (V_{bi}-V_{GS})^{\frac{3}{2}} + \frac{1}{\sqrt{1+N_d/N_{to}}}\left((U_{bi}+V_{DS})^{\frac{3}{2}} - U_{bi}^{\frac{3}{2}}\right)\right]\right\} \quad (1)$$

where,

$$V_{bi} = (kT/q)\ln(N_d/n_i), \text{ and} \quad (2)$$

$$U_{bi} = (kT/q)\ln\left(N_d N_{to}/n_i^2\right), \quad (3)$$

are the built-in potentials at the gate contact and across the n-GaN/SI-GaN interface respectively, N_d is the channel doping concentration, N_{to} is the trap concentration at the n-GaN channel/SI-GaN buffer interface, n_i is the intrinsic carrier concentration, ε is the GaN dielectric constant, q is the electronic charge, k is the Boltzman constant, T is the temperature in K, d is the thickness of the channel, W is

0-7803-7239-5/02/$10.00 © 2002 IEEE

the width and L is the gate length. The intrinsic parameters are obtained from:

$$g_m' = \partial I_D/\partial V_{GS}\big|_{V_{DS}},\ R_{ds}' = 1/\partial I_D/\partial V_{DS}\big|_{V_{GS}} \quad (4)$$

$$C_{gs} = C_{gs0}\left(1 - V_{GS}/V_{bi}\right)^{-\frac{1}{2}}, \text{ and} \quad (5)$$

$$C_{dg} = C_{dg0}\left(1 - V_{DG}/V_{bi}\right)^{-\frac{1}{2}}, \quad (6)$$

where, $C_{gs0} = C_{gd0} = 0.5WL\left(\varepsilon q N_d/2V_{bi}\right)^{\frac{1}{2}}$.

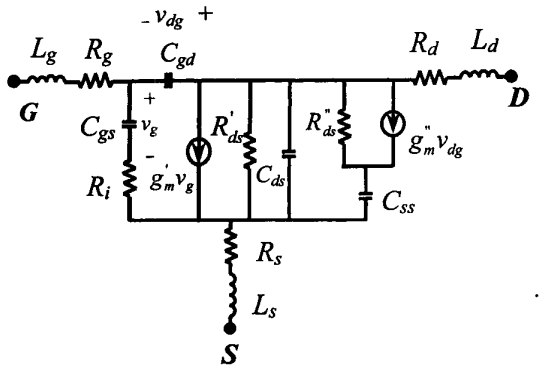

Fig.1. GaN MESFET large signal model. Linear model parameters are R_g = 6 Ω, L_g = 0.055 nH, R_d = 70 Ω, L_d = 0.307 nH, R_s = 90 Ω, L_s = 0.027 nH, R_i = 25 Ω and C_{ds} = 0.040 pF [6].

g_m'', C_{ss} and R_{ds}'' in Fig.1 are used to model the frequency dispersion of output conductance and transconductance due to traps and are given by,

$$g_m'' \approx q v_{sat} W d N_{to} \alpha \exp\left(-\alpha V_{DS}\right), \quad (7)$$

$$C_{ss} \approx C_{gs}, \quad (8)$$

$$R_{ds}'' \approx t_d/\left|C_{ss}\left(1 - g_m'' R_{ds}'\right)\right|, \quad (9)$$

where t_d is the detrapping time.

At any given frequency the overall intrinsic output conductance, g_{ds}, and transconductance, g_m, are obtained by analyzing the output subcircuit of Fig.1. For large-signal analysis, g_m, g_{ds} and C_{gs} are considered nonlinear functions of v_g while C_{gd} is nonlinear function of v_{dg}. The nonlinear functions are approximated up to second order term, $p = p_0 + p_1 v + p_2 v^2$, where p represents g_m, g_{ds}, C_{gs} or C_{gd} and v represents v_g or v_{dg}. The coefficients used in the expansions are shown in Table I for $L \times 150$ μm GaN MESFETs with d = 2000Å, $N_d = 2 \times 10^{17}$cm^{-3}, N_{to} = 1.5×10^{16} cm^{-3} and $\alpha = 0.112$ V^{-1}. The measured low field mobility μ_n is 410 cm^2 V^{-1}s^{-1} [4, 6].

For Volterra series analysis, the circuit in Fig.1 is terminated in a source impedance Z_S across gate-source and with a load impedance Z_L across drain-source. Defining ports 1 through 5 across nonlinear elements C_{gs}, g_m and g_{ds}, C_{dg}, load and source respectively, the elements of 5 × 5 system matrix Y are expressed as follows:

$$Y_{1,1}(\omega) = 1/R_i + j\omega C_{gs0}, \quad (10)$$

$$Y_{1,2}(\omega) = Y_{1,3}(\omega) = Y_{3,1}(\omega) = -1/R_i, \quad (11)$$

$$Y_{2,1}(\omega) = -1/R_i + g_{m0}, \quad (12)$$

$$Y_{1,4}(\omega) = Y_{4,1}(\omega) = Y_{1,5}(\omega) = Y_{5,1}(\omega) = 0, \quad (13)$$

$$Y_{2,2}(\omega) = 1/R_i + \left[\left\{1/\left(R_d + j\omega L_d\right) + 1/\left(Z_s(\omega) + R_g + j\omega L_g\right)\right\}^{-1} + R_s + j\omega L_s\right]^{-1}, \quad (14)$$
$$+ j\omega C_{ds} + g_{ds0}$$

$$Y_{4,4}(\omega) = \left[\left\{1/\left(Z_s(\omega) + R_g + j\omega L_g\right) + 1/\left(R_s + j\omega L_s\right)\right\}^{-1} + R_d + j\omega L_d\right]^{-1} + 1/Z_L(\omega), \quad (15)$$

$$Y_{5,5}(\omega) = \left[\left\{1/\left(R_s + j\omega L_s\right) + 1/\left(R_d + j\omega L_d\right)\right\}^{-1} + Z_s(\omega) + R_g + j\omega L_g\right]^{-1}, \quad (16)$$

$$Y_{2,5}(\omega) = Y_{5,2}(\omega) = -Y_{5,5}(\omega).\left[\left(R_d + j\omega L_d\right)/\left(R_s + j\omega L_s + R_d + j\omega L_d\right)\right], \quad (17)$$

$$Y_{2,4}(\omega) = Y_{4,2}(\omega) = \left|1/Z_L(\omega) - Y_{4,4}(\omega)\right| \left[\frac{Z_s(\omega) + R_g + j\omega L_g}{R_s + j\omega L_s + Z_s(\omega) + R_g + j\omega L_g}\right], \quad (18)$$

$$Y_{3,4}(\omega) = Y_{4,3}(\omega) = \left|Y_{4,4}(\omega) - 1/Z_L(\omega)\right| \left[\frac{R_s + j\omega L_s}{R_s + j\omega L_s + Z_s(\omega) + R_g + j\omega L_g}\right], \quad (19)$$

$$Y_{2,3}(\omega) = Y_{3,2}(\omega) = 1/R_i - Y_{2,5}(\omega), \quad (20)$$

$$Y_{3,3}(\omega) = Y_{5,5}(\omega) + 1/R_i + j\omega C_{dg0}, \quad (21)$$

$$Y_{3,5}(\omega) = Y_{5,3}(\omega) = -Y_{5,5}(\omega), \text{ and} \quad (22)$$

TABLE I

NONLINEAR MODEL PARAMETERS (V_{GS} = –4 V AND V_{DS} = 25 V) [6]

	L = 0.6μm	L = 0.8μm	L = 1.0μm		L = 0.6μm	L = 0.8μm	L = 1.0μm
g_{m0} (mS)	43.4	32.5	26.0	C_{gs0} (fF)	133.6	178.2	222.7
g_{m1} ($mS.V^{-1}$)	8.8	6.6	5.3	C_{gs1} (fF.V^{-1})	25.0	33.4	41.7
g_{m2} ($mS.V^{-2}$)	0.40	0.30	0.24	C_{gs2} (fF.V^{-2})	2.10	2.80	3.50
g_{ds0} (mS)	8.5	6.4	5.1	C_{gd0} (fF)	21.5	28.7	35.9
g_{ds1} ($mS.V^{-1}$)	2.7	2.0	1.5	C_{gd1} (fF.V^{-1})	–0.49	–0.66	–0.82
g_{ds2} ($mS.V^{-2}$)	0.21	0.16	0.13	C_{gd2} (fF.V^{-2})	0.005	0.007	0.009

$$Y_{5,4}(\omega) = Y_{4,5}(\omega) = -Y_{3,4}(\omega). \quad (23)$$

With an applied signal of amplitude V_{s1} and frequency ω_1, voltages across ports 1 through 4 are determined using [9]:

$$[V_p(\omega_1)] = -[Y_{i=p,j=1,\cdots,4}]^{-1}[Y_{i=p,j=5}]^T[V_{5,1,q} = V_{s1}], \quad (24)$$

where p = 1,...,4. The second-order voltages appear across ports at mixing frequencies, $\omega_{2,k} = \omega_1 + \omega_2$ when two tones are applied with amplitudes V_{s1} and V_{s2} and frequencies ω_1 and ω_2. Second-order port voltages are calculated by applying nonlinear currents through each nonlinear port. The nonlinear currents are evaluated using first-order port voltages due to individual tones and p_1 coefficients of nonlinear elements [9]. With Y matrix evaluated at mixing frequencies, the second-order port voltages are given by,

$$[V_p(\omega_1,\omega_2)] = -[Y_{i=p,j=1,\cdots,4}]^{-1}[I_{i=p,2,k}]^T, p = 1,\cdots,4. \quad (25)$$

Similarly, third-order port voltages due to tone amplitudes V_{s1}, V_{s2} and V_{s3} and frequencies ω_1, ω_2 and ω_3 are calculated by applying current sources due to nonlinear coefficients p_1 and p_2 and first and second-order port voltages. Then first, second and third order transfer functions are given by,

$$H_1(\omega_1) = V_4(\omega_1)/[V_{s1}Z_L(\omega_1)], \quad (26)$$

$$H_2(\omega_1,\omega_2) = 2\frac{V_4(\omega_1,\omega_2)}{V_{s1}V_{s2}Z_L(\omega_1,\omega_2)}, \text{ and} \quad (27)$$

$$H_3(\omega_1,\omega_2,\omega_3) = 4\frac{V_4(\omega_1,\omega_2,\omega_2)}{V_{s1}V_{s2}V_{s3}Z_L(\omega_1,\omega_2,\omega_3)}. \quad (28)$$

With two equal amplitude tones at frequencies ω_1 and ω_2, the third-order intermodulation components appear at $2\omega_1 - \omega_2$ and $2\omega_2 - \omega_1$. The output power and third-order intermodulation distortion are given by,

$$P_{out} = 0.5|V_4(\omega_1)/Z_L(\omega_1)|^2 \,\mathrm{Re}[Z_L(\omega_1)] \text{ and} \quad (29)$$

$$IM3 = 20\log_{10}\left[\frac{3}{4}V_{s1}V_{s2}\frac{|H_3(\omega_1,\omega_1,-\omega_2)|}{|H_1(\omega_1)|}\right]. \quad (30)$$

III. RESULT AND DISCUSSION

Fig.2 shows the calculated results of short-circuit current gain, |h21|, maximum stable gain, MSG, and maximum available gain, MAG for a 0.8 μm × 150 μm GaN MESFET. The calculated results are compared with experimental data to show good agreement. |h21| is 29 dB at 0.2GHz and drops to 0 dB at 6.5 GHz which corresponds to the gain-bandwidth product or the unity gain cut-off frequency, f_T of the device. MAG drops to 0 dB at 13 GHz which is the maximum frequency of oscillation, f_{max} of the device.

Fig.3 shows the fundamental and third-order output powers as a function of input power for 1.0 μm, 0.8 μm and 0.6 μm gate length GaN MESFETs with tones are at 1 GHz and 1.01 GHz. With increasing input power, the fundamental component of the output power becomes sub-linear as the device nonlinearity increases the other output power components. 1-dB compression point ($P_{1\text{-dB}}$) is referred to as the input power at which output deviates from linearity by 1 dB. $P_{1\text{-dB}}$ for 1.0 μm gate length device is 18 dBm and increases to 19.6 dBm for the 0.6 μm gate length device. Output referred third-intercept points (OIP3) are defined as the output power at which the third-order intermodulation components of the output power cross the fundamental component. OIP3 for 1.0 μm gate length device is 25.3 dBm and increases to 30.5 dBm in the 0.6 μm gate length device. These show a significant improvement in device linearity with decreasing gate length which can be correlated to the increasing device

transconductance and decreasing intrinsic capacitances (Table 1) with the reduction of gate length. These result in a better linearity in shorter gate length devices.

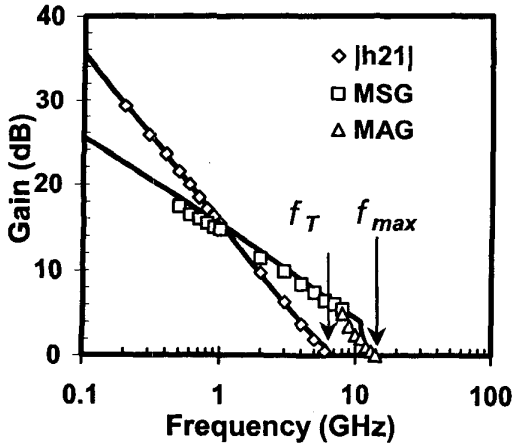

Fig.2. Calculated (solid lines) and measured (dots) short-circuit current gain $|h_{21}|$, maximum stable and available gains MSG and MAG of 0.8 μm gate length GaN MESFET [6].

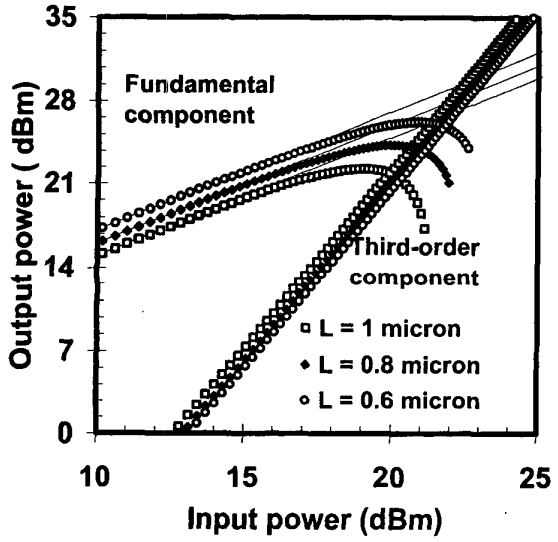

Fig.3. Calculated fundamental and third-order components of output power of $L \times 150$ μm GaN MESFETs [6].

Fig.4 shows the third-order intermodulation distortion (IM3) as a function of output power for 1.0 μm, 0.8 μm and 0.6 μm gate length GaN MESFETs. At 20 dBm output power, IM3 for 0.6 μm gate length device is −31 dBc and increases to −22 dBc for the 1.0 μm gate length device. This is due to the improvement in device linearity for shorter gate length devices as explained above.

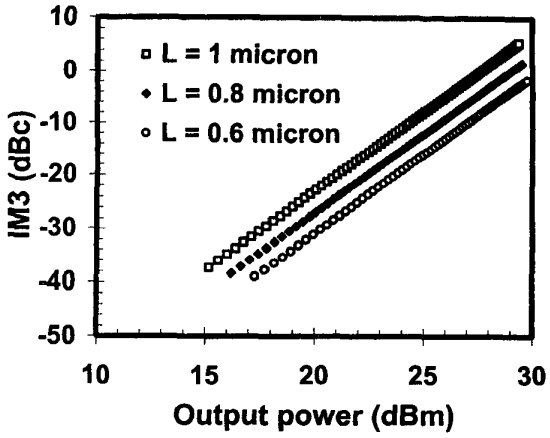

Fig.4. Third-order intermodulation (IM3) as a function of output power of $L \times 150$ μm GaN MESFETs [6].

IV. CONCLUSIONS

A physics-based large-signal model and nonlinearities of a GaN MESFET are reported. The model incorporated current collapse and frequency dispersion of output resistance and transconductance. The calculated results are in excellent agreement with the experimental data and verify the model in both dc and RF operation. Device nonlinearities are reported using Volterra series analysis. Significant improvement in device linearity is observed for shorter gate length devices.

REFERENCES

[1] Y.-F. Wu *et al.*, *IEEE Trans. on Electron Dev.*, Vol.48 (3), p.586, Mar. 2001.

[2] W. Lu *et al.*, *IEEE Trans. on Electron Dev.*, Vol.48 (3), p.581, Mar. 2001.

[3] I. Daumiller *et al.*, *Device Res. Conf. Dig.*, p.114, 1998.

[4] P.B. Klein *et al.*, *J. of Appl. Phys.*, Vol. 88 (5), p. 2843, Sept. 2000.

[5] K. Kunihiro *et al.*, *IEEE Electron Dev. Lett.*, Vol. 20 (12), p. 608, Dec. 1999.

[6] S.C. Binari *et al.*, *Solid-State Electronics*, Vol. 41 (10), p.1549, Oct. 1997.

[7] J.M. Golio *et al.*, *IEEE Trans. on Electron Dev.*, Vol. 37 (5), p. 1217, May 1990.

[8] T. Ytterdal *et al.*, *IEEE Trans. on Electron Dev.*, Vol. 46 (8), p.1577, Aug. 1999.

[9] S.A. Mass, *Nonlinear microwave circuits*, Norwood, MA: Artech House, 1988.